Palmprint Recognition Using Neighboring Direction Indicator

Lunke Fei, *Student Member, IEEE*, Bob Zhang, *Member, IEEE*, Yong Xu, *Senior Member, IEEE*, and Liping Yan

***Abstract*—Orientation features are successfully used in coding-based palmprint recognition methods. In this paper, we propose a discriminative neighboring direction indicator to represent the orientation feature of the palmprint. The neighboring direction indicator feature not only represents the most dominant orientation feature of the palmprint, but also better describes the orientation feature of those points which have double dominant orientations. In addition, the neighboring direction indicator shows good robustness to noise and rotation. Using the neighboring direction indicator, we propose a novel palmprint recognition method. Extensive experiments conducted on three types of palmprint databases demonstrate that the proposed method gives better performance than the existing state-of-the-art orientation-based methods. By using the proposed method, the equal error rate is improved by about 10% for palmprint verification, and the average error rate is reduced by 2.7–14% for palmprint identification with a single training sample.**

***Index Terms*—Biometric, multiple orientation representation, neighboring direction indicator, palmprint recognition.**

I. Introduction

HUMANS have been successfully using biometrics of face, iris, fingerprint, voice, and gait for personal authentication. As a relatively new biometric authentication technology, palmprint recognition has considerable potential, because it possesses most of the discriminative features of fingerprints, such as minutiae points, singular points, and texture, besides other special features, such as principal lines, wrinkles, and ridges [1]–[4]. By virtue of these features, palmprint-based recognition can give results. Consequently, in recent years, increasing interest is being shown in the research of this new promising field [5]–[8].

So far, line, texture, minutiae point, appearance, and multifeature-based palmprint recognition methods have been studied extensively. For example, Huang, Jia, and Zhang [9] extract the principle lines from palmprints for matching. In [10], the authors extract more palm lines, including both principal lines and wrinkles, for palmprint authentication. Zhang, Kong, You, and Wong [11] propose an effective palmprint identification method based on the texture of the palmprint. Morales, Ferrer, and Kumar [12] propose contactless palmprint verification, using the scale-invariant feature transform points of the palmprint. In [13], a high-resolution palmprint recognition algorithm, using the statistics of ridges of the palmprint, is proposed. In [14], Chen, Huang, and Zhou present a hierarchical minutiae matching algorithm for palmprint identification with high accuracy. The minutiae features of the palmprint are successfully used for matching latent palmprint image for forensic applications [15]. Roux, Aoyama, Ito, and Aoki [16] and Badrinath and Gupta [17] apply the phase information of a palmprint to design a palmprint recognition algorithm. At the same time, much attention has been directed toward the fusion of multiple features of palmprint. Li, Zhang, Zhang, Lu, and Yan [18] design a palmprint recognition method using the 2-D and 3-D palmprint features. Zhang, Guo, Lu, Zhang, and Zuo [19], [20] provide a multispectral palmprint recognition method that captures the palmprint under red, green, blue, and near-infrared (NIR) light and then fuse them at the image or matching score level to improve the performance of palmprint recognition. Xu, Fei, and Zhang [21] propose a multimodal-based personal identification method by combining the left and right palmprints. In [6], a rank-level fusion scheme is proposed for multibiometrics combination. In [22], Dai and Zhou propose a multifeature-based method, which extracts and compares the minutia points, orientation, density map, and principal lines. Besides the above methods, subspace-based methods, such as the Eigenpalm [23], Fisherpalm [24], locality preserving projections [25], Fisher discriminant analysis, and independent component analysis [26], are also proposed and applied for palmprint recognition.

Zhang, Kong, You, and Wong [11] implement an online system for palmprint identification. The system utilizes a normalized 2-D Gabor filter to extract the orientation feature of palmprint, called palmcode, and achieves satisfactory performance in real-time palmprint application. Since then, the coding-based methods have been developing rapidly. Kong and Zhang [27] propose a principal orientation-based method, named competitive code, which uses six Gabor filters of different orientations to extract the dominant orientation of a palmprint based on the principle of the winner-take-all. The competitive code method is probably the most promising coding method in palmprint recognition. Inspired by the competitive code method, Kong, Zhang, and Kamel [28] propose the fusion code method

Manuscript received December 29, 2015; revised April 13, 2016; accepted June 24, 2016. Date of publication July 18, 2016; date of current version November 11, 2016. This work was supported in part by the National Natural Science Foundation of China (NSFC) under Grant 61370163, in part by the GRF Fund from the HKSAR Government, in part by the Central Fund from Hong Kong Polytechnic University, and in part by the NSFC Overseas Fund (61020106004), China. This paper was recommended by Associate Editor A. Basu.

L. Fei and Y. Xu are with the Bio-Computing Research Center, Shenzhen Graduate School, Harbin Institute of Technology, Shenzhen 518055, China (e-mail: flksxm@126.com; laterfall2@yahoo.com.cn).

B. Zhang is with the Department of Computer and Information Science, University of Macau, Taipa, Macau (e-mail: bobzhang@umac.mo).

L. Yan is with the Computer Application Research Institute, Computer School, Wuhan University, Wuhan 430072, China (e-mail: csyan@whu.edu.cn).

Color versions of one or more of the figures in this paper are available online at http://ieeexplore.ieee.org.

Digital Object Identifier 10.1109/THMS.2016.2586474

that encodes the phase of filtering result with the maximum magnitude among four filters. Based on a rule that is similar to the winner-take-all rule, the robust line orientation code (RLOC) method [29] extracts principal orientation code of a palmprint by using a modified finite radon transform. Zuo, Lin, Guo, and Zhang [30] design a sparse multiscale competitive code method which can extract the orientation feature of a palmprint more accurately, using a bank of multiscale Gabor filters. To effectively obtain more orientation features of a palmprint, Guo, Zhang, Zhang, and Zuo [31] propose a binary orientation cooccurrence vector (BOCV) representation that binarizes all the filter responses of a palmprint image, convolving with Gabor filters on six orientations. To further explore the BOCV, Zhang, Li, and Niu [32] propose the E-BOCV method, which involves filtering out the fragile bits of the BOCV. In contrast with the coding methods mentioned above, Sun, Tan, Wang, and Li. [33] employ three groups of orthogonal Gaussian filters to extract ordinal measurement-based codes of a palmprint.

This paper proposes a novel and efficient orientation representation method, called neighboring direction indicator. This method has the following advantages. First, the neighboring direction indicator essentially means the most dominant orientation of the palmprint, which can better represent those points that have double dominant orientations. Second, it shows good robustness to noise and rotation. Third, it has a simple and effective balancing scheme to improve the precision of the orientation feature of the palmprint. Finally, extensive experiments carried out on three baseline palmprint databases show that the results obtained by the proposed method for palmprint verification and identification are more accurate than those obtained by any the state-of-the-art orientation-based methods. Moreover, the proposed method gives the most competitive performance in multispectral palmprint verification.

The remainder of this paper is organized as follows. Section II briefly reviews the popular orientation-based methods. Section III introduces the neighboring direction indicator of palmprint, based on which, we propose, in Section IV, a simple and effective algorithm for palmprint recognition. In Section V, a series of experimental results are reported and analyzed. Finally, Section VI sums up the conclusion drawn from this study.

II. Related Work

In this section, several state-of-the-art coding-based palmprint recognition methods are reviewed. In general, coding-based methods use one or several filters to extract the orientation features of a palmprint image and then convert them into binary codes. Usually, the distance metric is used to evaluate the similarity between code features.

The palmcode method uses a 2-D Gabor filter with orientation of $\pi/4$ to extract the orientation feature of a palmprint and then convert it into a pair of binary codes. The competitive code method uses six Gabor filters with different orientations, $j\pi/6(j = 0, 1, ..., 5)$, to extract one dominant orientation feature from a palmprint. In other words, six Gabor templates are first convoluted with the palmprint image. The orientation of the Gabor filter with the maximum response is finally determined as the dominant orientation feature of the palmprint, whose index is taken as the competitive code. For example, the index of the orientation $j\pi/6$ is defined as j, where $j = 0, 1, ..., 5$. The angular distance metric is used for comparing two competitive codes. The angular distance of two orientations is based on the following rules: between parallel orientations, the distance is 0; when the angles of the two orientations are $\pi/6$ and $5\pi/6$, the distance is 1; when they are $2\pi/6$ and $4\pi/6$, the distance is 2; and between perpendicular orientations, the distance is 3. To speed up the calculation of the angular distance, the competitive code can be binarized into 3-bit codes via the rule in [28]. Then, the normalized Hamming distance can be used to calculate the angular distance between two competitive code maps.

Similar to the competitive code method, both RLOC and fusion code methods adopt the winner-take-all rule to extract a single dominant orientation feature of a palmprint. In addition, the RLOC method designs a set of special convolution templates, and the fusion code method uses four orientations of Gabor filters.

Unlike the single orientation code-based method, the BOCV and EBOCV methods try to obtain multiple orientation features of a palmprint. Both the BOCV and EBOCV methods use six Gabor filters with orientations of $j\pi/6(j = 0, 1, ..., 5)$ to convolve with a palmprint image. The signs of the filter responses on all the six orientations are binarized. Thus, 6-bit code planes can be formed for a palmprint. In contrast with the BOCV method, the EBOCV method filters out the fragile bits from the code planes of the BOCV. A normalized Hamming distance metric is finally used to measure the dissimilarity between the code planes of two palmprint images.

By appropriately comparing the filtering results on two orientations, Sun, Tan, Wang, and Li [33] propose an ordinal coding method, which essentially incorporates three groups of Gaussian filters. Each incorporated filter consists of two perpendicular 2-D Gaussian filters with orientations of $j\pi/6$ and $(j + 3)\pi/6$, where $j = 0, 1, 2$. Three incorporated Gaussian filters are convolved with a palmprint image. The signs of filtering results are encoded into 3-bit binary codes, and then, the Hamming distance between two ordinal code planes is calculated in the matching stage.

In these coding methods, different feature extraction schemes are used, each extracting a different number of code features. As a result, if the dominant orientation feature of a palmprint alone is extracted, the other orientation features of the palmprint will be lost. If all the orientation features of a palmprint are preserved equally, the importance of the dominant orientation of the palmprint is weakened. Against the background of these two extreme situations, the fundamental question that arises is how to design a more accurate scheme that better represents palmprint orientation features? This question forms the starting point of this paper.

III. Neighboring Direction Indicator

It is well known that the orientation feature of a palmprint is successfully used in palmprint recognition. By simply coding the orientation feature of a palmprint, palmprint recognition with

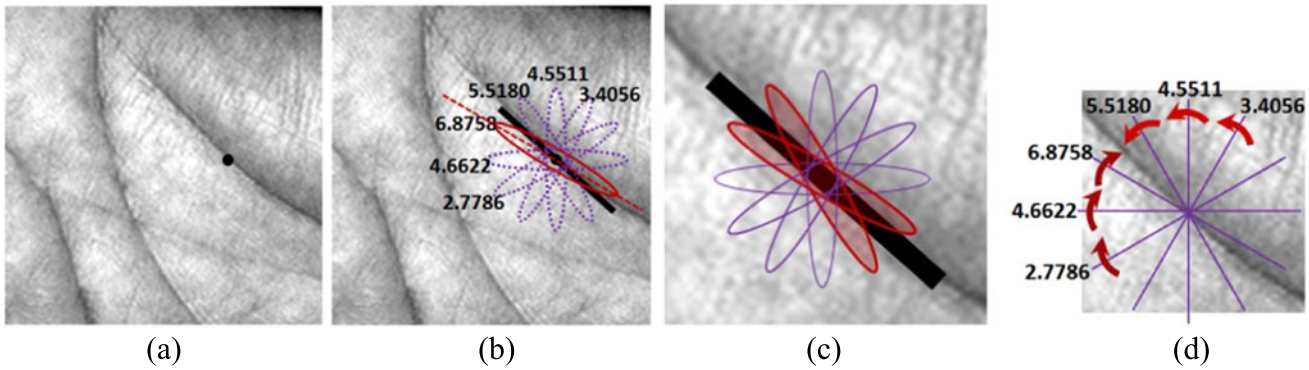

Fig. 1. Procedure for orientation extraction. (a) Original palmprint image. (b) Orientation feature extraction by convolving the palmprint (a) with six filters. (c) Two filters that usually produce larger filter responses than others. (d) Using the neighboring direction indicator to represent the orientation features of the palmprint.

high accuracy can be achieved. The competitive code method is probably the most promising method among all the orientation-based methods [1], which uses six Gabor filters with different orientations to convolve a palmprint image. The orientation of the filter that generates the maximum filter response with the palmprint image is treated as the dominant orientation of the palmprint. However, in real operation, only a bank of Gabor filters with discrete orientations are adopted. Thus, the orientation of the filter that has the largest filter response is usually not the real dominant orientation of the palmprint but just the one near it. The extraction of the dominant orientation is illustrated in Fig. 1. Fig. 1(a) and (b) shows that a point with obvious principal orientation is selected to convolve with six discrete Gabor filters and the corresponding filter results. From Fig. 1(b), we can see that the dominant orientation extracted by the competitive code method is the orientation of the Gabor filter with maximum filter response, e.g., $5\pi/6$. Actually, the orientation of the Gabor filter with the maximum filtering result just approximates the principal orientation of the point illustrated in Fig. 1(a).

Fig. 1(c) shows two neighbor orientations of Gabor filters, which are near the genuine principal orientation. The filter responses of these two neighbor orientations are almost always larger than those of other orientations. In fact, a similar situation can be observed on other orientations too. That is, each orientation of the six Gabor filters has two neighbor orientations. The neighbor orientation, which is nearer to the principal orientation than others, can produce a larger filter response. A neighboring direction indicator can be used to identify the side of the larger filter response between the two neighbor filters. Further, as shown in Fig. 1(d), the neighboring direction indicator can be extracted on all the six orientations, and thus, 6-bit code planes can be obtained from a palmprint. A clockwise indicator represents that the filter response of the right-side neighbor is larger than that of the left-side neighbor; otherwise, a counterclockwise indicator is represented. Since the neighboring direction indicators always point to the side of the orientation with the larger filter response, they essentially constitute the information of the most dominant orientation of the palmprint. By using the neighboring direction indicator, a novel method is proposed for palmprint recognition.

IV. Neighboring Direction Indicator-Based Method

A. Palmprint Preprocessing

Palmprint preprocessing is executed before palmprint feature extraction. The goal of preprocessing is to extract the region of interest (ROI) [34] from palmprint image. The method proposed in [11], which extracts the central region of the palmprint, is employed in our method. We first use the low-pass Gaussian filter to convolve the original palmprint image and convert the convolved image into a binary image by thresholding the resultant convolved image and obtain the boundaries of the binary image by using a boundary tracking algorithm. Then, we use the gaps between fingers as reference points to determine the ROI of the palmprint. In other words, we determine the landmarks based on the boundaries, which are at the bottom of the gaps between index and middle fingers and between the ring and little fingers. The line connecting these two landmarks is considered to be tangential to them. After that, we locate the bisector that is perpendicular to the tangent between two landmarks to determine the centroid of the palmprint region. Finally, we extract the normalized subimage of a fixed size, i.e., 64×64, as the ROI, which is located in a certain area of the palmprint. Fig. 2 shows the procedure for extracting the ROI of a palmprint image.

B. Neighboring Direction Indicator Extraction and Matching

Filters, such as Gabor, Randon, Gaussian, and anisotropy filters [35], are used to extract orientation features of a palmprint in coding-based methods [1]. Of them, the Gabor filter is the most appropriate one for capturing the orientation information from palm lines [36], [37]. This is mainly because it has good properties of 2-D spectral specificity of textures as well as their variations with 2-D spatial position. Further, Xue, Zuo, and Wang [38], after comparing the performances of coding-based methods by using different filters, conclude that Gabor filter gives the best performance. Since the neighboring direction

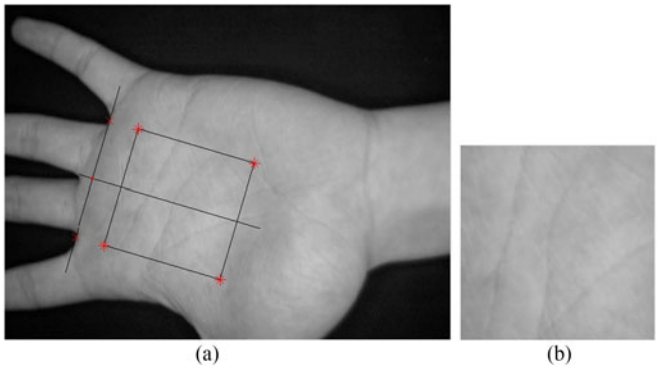

Fig. 2. ROI extraction of a palmprint image. (a) Original palmprint image. (b) ROI extracted from (a).

indicator is based on the orientation feature of the palmprint, we apply the Gabor filter to calculate the neighboring direction indicator of palmprint image also. The typical circular Gabor filter has the following general form:

$$G(x,y,\theta,\mu,\sigma) = \frac{1}{2\pi\sigma^2}\exp\left\{-\left(\frac{x^2+y^2}{2\sigma^2}\right)\right\} \exp(i2\pi\mu(x\cos\theta + y\sin\theta)) \quad (1)$$

where $i=\sqrt{-1}$, μ is the radial frequency in radians per unit length, θ is the orientation of the Gabor function in radians, and σ is the standard deviation of the elliptical Gaussian along x- and y-axes, respectively. Following [11], the parameters are empirically set as $\mu = 0.0916$, and $\sigma = 5.6179$. The real part of the Gabor filter is used to extract the neighboring direction indicator of the palmprint image.

We find that six Gabor filters is the optimal requirement for orientation extraction of the palmprint [31]. Therefore, six Gabor filters with orientation of $j\pi/6(j=0,1,...,5)$ are also employed to extract the neighboring direction indicator of the palmprint. They are first used particularly to convolve with the palmprint image. Let G_j^r be the real part of G with orientation $j\pi/6(j=0,1,...,5)$. The convolution of the palmprint image with G^r is

$$R_j(x,y) = G_j^r * I(x,y), \quad (j=0,1,...,5) \quad (2)$$

where I denotes the palmprint image, and "*" the convolution operation. $R_j(x,y)$ is the convolution result of $I(x,y)$ with G^r on orientation of $j\pi/6$. A small area of points in the palmprint usually has similar orientation features. To robustly extract the orientation feature, we update the original convolution results by convolving a smoothing filter as follows:

$$\bar{R}_j = W * R_j, \quad (j=0,1,...,5) \quad (3)$$

where W is the smoothing filter as shown in Fig. 3, and $\bar{R}$ is the updated convolution result, balancing the convolutions of the neighboring pixels.

The neighboring direction indicator of point $I(x,y)$ is determined, based on the updated filter responses of the two neighboring orientations of $j\pi/6$. Particularly, the neighboring direction indicator of the current orientation is encoded into 1,

$$\frac{1}{9}\times\begin{array}{|c|c|c|}\hline 1&1&1\\\hline 1&1&1\\\hline 1&1&1\\\hline\end{array}$$

Fig. 3. Smoothing filter for updating convolution results between the Gabor filters and palmprint images.

if the left-side neighbor filter response is larger than that of the right-side; otherwise, it is encoded into 0. Thus, the neighboring direction indicator code of orientation $j\pi/6$ can be calculated as

$$P_j(x,y) = \begin{cases} 1, & \text{if } \bar{R}_{j_{\text{left}}}(x,y) \geq \bar{R}_{j_{\text{right}}}(x,y) \\ 0, & \text{else} \end{cases} \quad (4)$$

where j is the orientation index of orientation $j\pi/6$, and j_{left} and j_{right} are indices of the neighboring orientations of $j\pi/6$ on the left and right sides, respectively. These two indices can be calculated as follows:

$$j_{\text{left}} = \begin{cases} j+1, & \text{if } 0 \leq j \leq 4 \\ 0, & \text{if } j = 5 \end{cases} \quad (5)$$

and

$$j_{\text{right}} = \begin{cases} j-1, & \text{if } 1 \leq j \leq 5 \\ 5, & \text{if } j = 0. \end{cases} \quad (6)$$

Since there are six different orientations on the whole, six indicator code planes have formed finally, which are denoted by $P_j(j=0,1,...,5)$, where P is regarded as the neighboring direction indicator code feature of the palmprint.

If P and Q are two neighboring direction indicator code planes, the normalized Hamming distance is used as follows, to determine their similarity:

$$D(X,Y) = \frac{\sum_{j=0}^{5}\sum_{x=1}^{N}\sum_{y=1}^{N}(P_j(x,y)\otimes Q_j(x,y))}{6N^2} \quad (7)$$

where $P_j(Q_j)$ is the jth bit plane of $P(Q)$, X and Y are original palmprint images of P and Q, N^2 is the size of palmprint image, and "$\otimes$" is the bitwise "exclusive OR" operation. Obviously, the range of D is from 0 to 1. If $D(X,Y)$ is small, it means that the similarity between X and Y is high. The hamming distance between two code maps is also called their matching score.

C. Analysis of the Neighboring Direction Indicator of Palmprint

Some examples are presented here to illustrate the robustness of the neighboring direction indicator of a palmprint image. From the pixels of a noisy palmprint image, one pixel is particularly selected to extract the neighboring direction indicator feature by using the proposed method and the dominant orientation, following the rule of winner-take-all. Fig. 4(a) and (b) shows the neighboring direction indicator features and the dominant orientation features extracted, respectively, from the original image and the noisy image, to which 0.02% "salt &

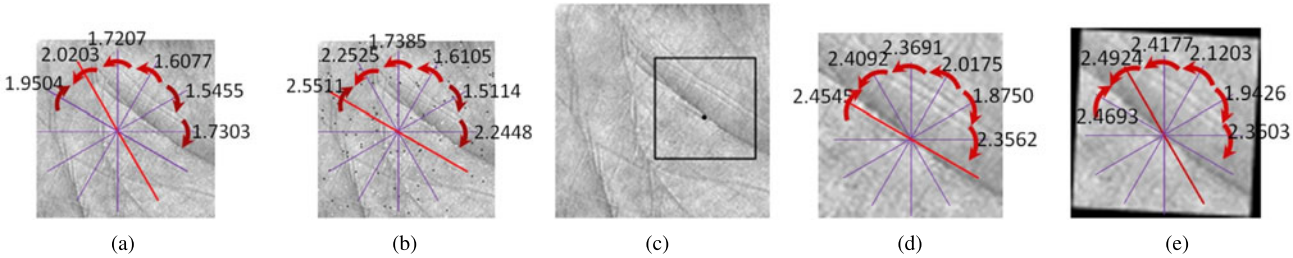

Fig. 4. Robustness of the neighboring direction indicator. The neighboring direction indicator features on (a) palmprint image and on (b) the same palmprint image with 0.02% "salt & pepper" noise added. (c) Example of the pixel that has one dominant orientation; the neighboring direction indicator features (e) on the palmprint image (d) and (f) on the rotated palmprint image. The red lines show the dominant orientations extracted based on the maximum response.

pepper" noise has been added. It can be seen that the dominant orientations, extracted based on the maximum response, have changed after adding the noise. This is mainly because the top two responses are very close to each other, and the maximum response is sensitive to the noise. On the contrary, the neighboring direction indicator feature can be stably extracted from both palmprint images. Furthermore, Fig. 4(f) shows a palmprint image that rotates anticlockwise by a small degree, say 3°. The dominant orientation of the pixel, extracted based on the maximum response, has changed from $5\pi/6$ to $4\pi/6$, after rotation. However, since the neighboring direction indicators usually point to the side of the real dominant orientation of the palmprint, they can be stably extracted from the rotated palmprint image. Therefore, the neighboring direction indicator feature of the palmprint is more robust to the noise and rotation than the conventional methods based on the winner-take-all rule.

In addition, we note that the pixels in a palmprint usually have two dominant orientations. For example, Fig. 5 shows some points in the palmprint image, which are within two crossing wrinkles. They obviously possess two dominant orientations. The conventional methods can roughly extract only one of the two dominant orientations, based on the winner-take-all rule for these points. By contrast, the neighboring direction indicator feature can better represent the double dominant orientations of these points by pointing out the side of these dominant orientations. Therefore, the neighboring direction indicator is suitable to extract the orientation feature of the palmprint.

D. Unified Framework for Ordinal Measurement-Based Method

Essentially, the code plane of the neighboring direction indicator extracted by the proposed method is based on the relationship between the filtering results of two orientations with an interval of $\pi/3$. We notice that the conventional ordinal code scheme is also based on the filtering results of two orientations with an interval of $\pi/2$. It is thus evident that the proposed method is similar to the ordinal measurement-based method [33]. Therefore, we propose a unified framework for the ordinal measurement-based method as follows:

$$P_j(x,y) = \begin{cases} 1, & \text{if } R_j(x,y) \geq R_{j_k}(x,y) \\ 0, & \text{else} \end{cases} \tag{8}$$

where

$$j_k = \begin{cases} j+k, & \text{if } (j+k) \leq 5 \\ (j+k) \bmod 5, & \text{else.} \end{cases} \tag{9}$$

In the unified framework, it must be mentioned that the range of k is from 1 to 3. The case with $k = 4$ is exactly the same as that of the one with $k = 2$. Both show that the interval between the two compared orientations is $\pi/3$. Similarly, the interval between two orientations is $\pi/6$ for both $k = 5$ and $k = 1$. $k = 3$ represents an orientation interval of $\pi/2$, which is similar to the conventional ordinal code method. In this study, the proposed method represents the case of the unified framework with $k = 2$.

It is noted that by using the conventional ordinal code method, only 3-bit ordinal codes are obtained. This is because the ordinal code extracted with $j(j = 3, 4, 5)$ is exactly opposite to that of $(j - 3)$ in the framework. In other words, the code feature extracted using $j(j = 3, 4, 5)$ is redundant. Thus, compared with the conventional ordinal code method, the proposed method can extract more ordinal measurement-based code planes, which suitably increases the discriminative power of the proposed method.

V. Experimental Results

In this section, we evaluate the verification and identification performance of the proposed method, using three types of popular palmprint databases: PolyU, IITD, and multispectral databases. The proposed method is compared with several state-of-the-art orientation-based methods and also an ordinal measurement-based method.

A. Palmprint Database

The PolyU database (version 2) [39] contains 7752 palmprint images collected from 193 individuals, among whom 131 were males and 62 females. The youngest individual was about ten years old and the oldest one about 55 years old. The palmprint images were collected in two sessions, separated by an average interval of over two months. In each session, about ten palmprint images were captured from the left and right palms of each individual. Thus, about 40 palmprint images (20 from each palm) were captured from each individual. Consequently, there were 386 classes of palm on the PolyU database, each with about 20 palmprint images. All the images were captured under

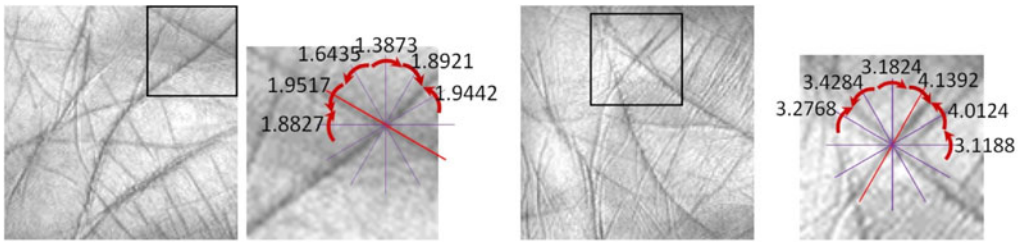

Fig. 5. Neighboring direction indicator representation of the pixel that has two dominant orientations. (a) and (c) represent two examples of pixels that have two dominant orientations. (b) and (d) depict the neighboring direction indicator feature of these pixels.

a user-pegs-based environment to restrict the hand-pose and image scale variations before extracting the ROI of the palmprint. Each palmprint image was cropped to a size of 128 × 128 pixels.

The IITD database was provided by the Biometrics Research Laboratory of IIT Delhi [40]. Compared with the PolyU database, it is a touchless-based palmprint database. Its images were captured by a camera in an indoor environment by employing circular fluorescent illumination around the camera lens and without using user-pegs setup. The database was collected from 230 individuals, who were in the age group of 12–57 years. Each of them contributed ten palmprint images: five from the left palm and five from the right palms. The IITD database thus consists of 2300 contactless palmprint images of 460 palms. Since there is no contact or guiding surface to restrict the hand movement while capturing palmprint image, the hands are highly variant in pose, projection, rotation, and translation. In other words, the images of IITD database have significant intraclass variations. The resolution of original images was 800 × 600 pixels. Cropped ROI images of 150 × 150 pixels are also available in the IITD database.

Palmprint images of multispectral palmprint database were captured under blue, green, red, and NIR illuminations. Thus, the multispectral database consists of four independent spectral palmprint databases: Red, Green, Blue, and NIR spectral [39]. Each database was collected from the left and right palms of 250 volunteers, among whom 195 were males and 55 females. Their age was in the range of 20–60 years. The palmprint images were acquired in two sessions, separated by a time interval of around one week. In each session, every subject was asked to provide six images of the left palm and six of right palm. Thus, each spectral database contains 6000 of 500 palms, each palm contributing 12 images. All palmprint images had been cropped to a size of 128 × 128 pixels.

For a better illustration of the differences between these palmprint images, some examples of ROIs of some palmprint images, selected from different types of palmprint databases, are shown in Fig. 6. The size of all the palmprint images was normalized to 64 × 64 pixels for the following experiments. It is observed that some ROI images were wrongly extracted from palmprint images, as shown in Fig. 7, mainly because of incorrect placement of the palm, while its image was being captured, resulting in the capture of redundant nonpalmprint region in the extracted ROI. One effective way of removing the redundant region is to locate the pixels of such black-region by defining a mask using thresholding [11]. From the public ROI databases [39], [40], we have observed that the rate of incorrect ROI detection is generally less than 1%. In our experiments, for fairness in comparison, all the methods were performed on the baseline ROI databases, without removing the black-regions.

B. Palmprint Verification

In verification experiments, the class of the palmprint images in a database is to be known so that each of them can be matched with other samples in the same database. A match is counted as genuine if both the samples are from the same palm; otherwise, the match is called as imposter. In other words, the genuine match is an intraclass comparison and the imposter match is an interclass comparison. The PolyU palmprint database has 7752 samples. So the total number of matches is 30 042 876 (7752 × 7751)/2), of which 74 068 are genuine matches and 29 968 808 imposter matches. In the IITD database, the total number of matches is 2 643 850 (2300 × 2299/2), of which 4600 are genuine matches and 2 369 250 imposter matches. In the multispectral database, each spectral subdatabase contains 17 997 000 (6000 × 5999/2) matches, of which 33 000 are genuine matches and 17 964 000 imposter matches.

Fig. 8 shows the distribution of genuine matching score and imposter matching score, obtained by using the proposed method on the PolyU database, IITD database, Red, Green, Blue, and NIR databases. It can been seen that the two scores can be easily distinguished in the PolyU and multispectral databases by using a linear classifier, but it is not so in the IITD database, because the palmprint images of this database show marked variations in rotation and projection. Nevertheless, the matching scores of genuine matches are usually smaller than those of the imposter matches.

To assess the performance of the proposed method, we conducted verification experiments using the proposed method and several state-of-the-art coding methods. Genuine acceptance rate (GAR) and false acceptance rate (FAR) were used to evaluate the performance. In addition, equal error rate (EER), the point where the false reject rate is equal to FAR, was also used. The receiver operating characteristic (ROC) curve, a graph of GAR versus FAR, for all possible decision thresholds, was introduced to compare the performance of different methods. The ROC curves of the proposed method on different palmprint databases are shown in Fig. 9. ROC curves obtained by using the

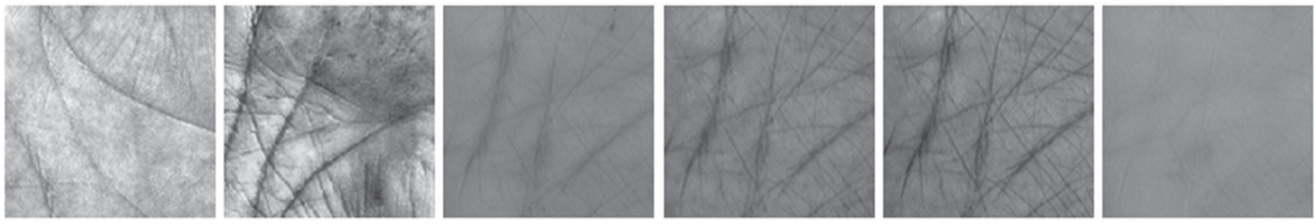

(a) (b) (c) (d) (e) (f)

Fig. 6. Examples of ROIs extracted from the palmprint images of three types of palmprint databases. (a)–(f) ROIs of the palmprint images from the PolyU, IITD, Red, Green, Blue, and NIR databases, respectively.

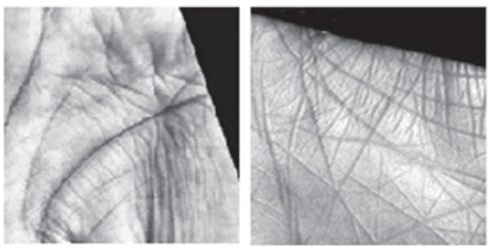

(a) (b)

Fig. 7. Examples of ROIs with redundant black-regions: ROIs containing nonpalmprint regions, extracted from palmprint images of (a) PolyU database and (b) IITD database.

current state-of-the-art coding methods, such as the competitive code, ordinal code, fusion code, palmcode, BOCV, E-BOCV, and RLOC methods, are also plotted in Fig. 9. From these figures, we see that, against the same FAR, the proposed method achieves the highest GAR among all the coding methods.

The EERs of different methods, summarized in Table I, illustrate that the proposed method obtains the lowest EER on all the three palmprint databases. For example, for the PolyU database, the lowest EER achieved by other coding methods is 0.0261%, which is 13.79% ((0.0261-0.0225)/0.0261) higher than the EER obtained by the proposed method. For the IITD database, the EER of the proposed method is 14.65% lower than the best EER of other coding methods. On the multispectral palmprint databases also, the proposed method performs consistently better than other methods.

C. Palmprint Identification

Identification is a one-against-many comparison process which tries to classify the palmprint image being probed into the correct class index. In palmprint identification experiments of this study, we first used $N(N = 1, 2, ...)$ palmprint image(s) from each palm as the training sample. Then, the remaining palmprint images from each palm form the testing set. Since each class of palm contains $N(N = 1, 2, ...)$ training image(s), each testing sample will generate N matching score(s). The minimum of each is regarded as the final matching score between the testing sample and the class. As a result, each testing sample will generate C matching scores, where C is the class number of the training samples. In the final decision, the class of the training sample, which produces the minimum of C matching scores, is taken as the class of the testing sample. The identification error rate, i.e., the ratio of the number of the testing samples that are classified into incorrect classes to the total number of testing samples, is used to estimate the accuracy of the palmprint identification.

To compare our method with other coding methods for palmprint identification, we also implemented several state-of-the-art coding-based methods, such as the competitive code, ordinal code, fusion code, palmcode, BOCV, E-BOCV, RLOC, and DR+CS [35] methods. We repeated the identification experiment five times by using one to five training samples from each palm. It should be pointed out that there are only five palmprint images for each palm in the IITD database. Therefore, only four tests were run. The experimental results obtained on the three types of palmprint databases are depicted in Fig. 10. Table II details the identification results with $N = 1$. From the table, it is not hard to see that the proposed method decreases the error rate of the palmprint identification significantly. For example, the average palmprint identification improvement of the proposed method reaches about 5.57% on the PolyU database. The average improvement is about 14% on the IITD database. On the four spectral databases, the average improvements are about 2.74%, 3.67%, 3%, and 4.35%.

D. Effectiveness in Multispectral Palmprint Verification

To further evaluate the effectiveness of the neighboring direction indicator representation, we apply the proposed method to the multispectral palmprint verification and compare it with the state-of-the-art multispectral palmprint fusion method [19]. It is noted that the fusion of Red and Blue bands can achieve the best result for palmprint verification. In addition, the fusion of Red, Blue, and NIR bands, as well as the fusion of Red, Blue, Green, and NIR bands, can also achieve comparable results. Therefore, these three optimal band groups are employed for our comparison. Particularly, we use the proposed method to perform feature extraction and matching on each band and then to fuse the matching results on different bands at matching score level, where the weight $w = 1/\text{EER}$ for each band [19]. The experimental results obtained by using the method in [19] and those obtained by using the proposed method are summarized in Table III. It can be seen that the proposed method can achieve much lower EER than does the method in [19] on each combination of bands. This is possibly because the proposed method can not only extract the single dominant orientation, but also

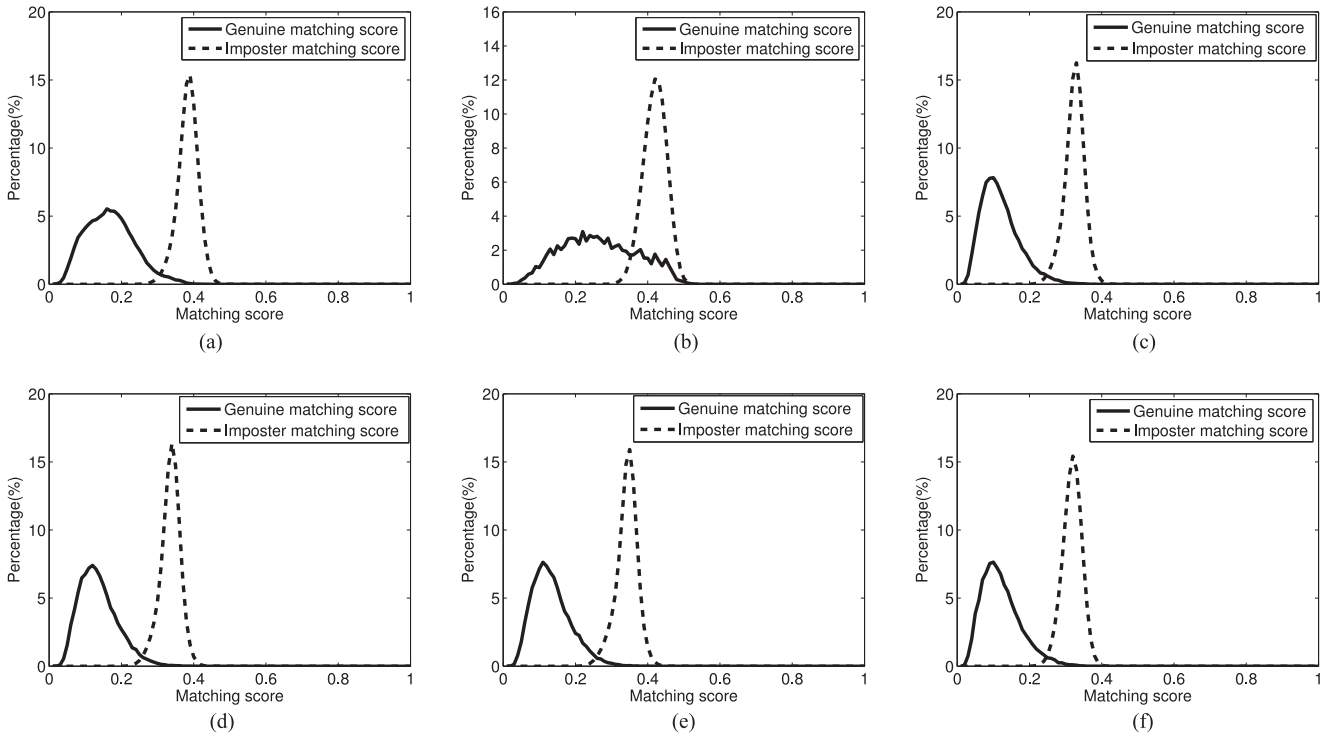

Fig. 8. Distribution of matching scores obtained by using the proposed method. (a)–(f) Distributions of genuine and the imposter matching scores on the PolyU, IITD, Red, Green, Blue, and NIR databases, respectively.

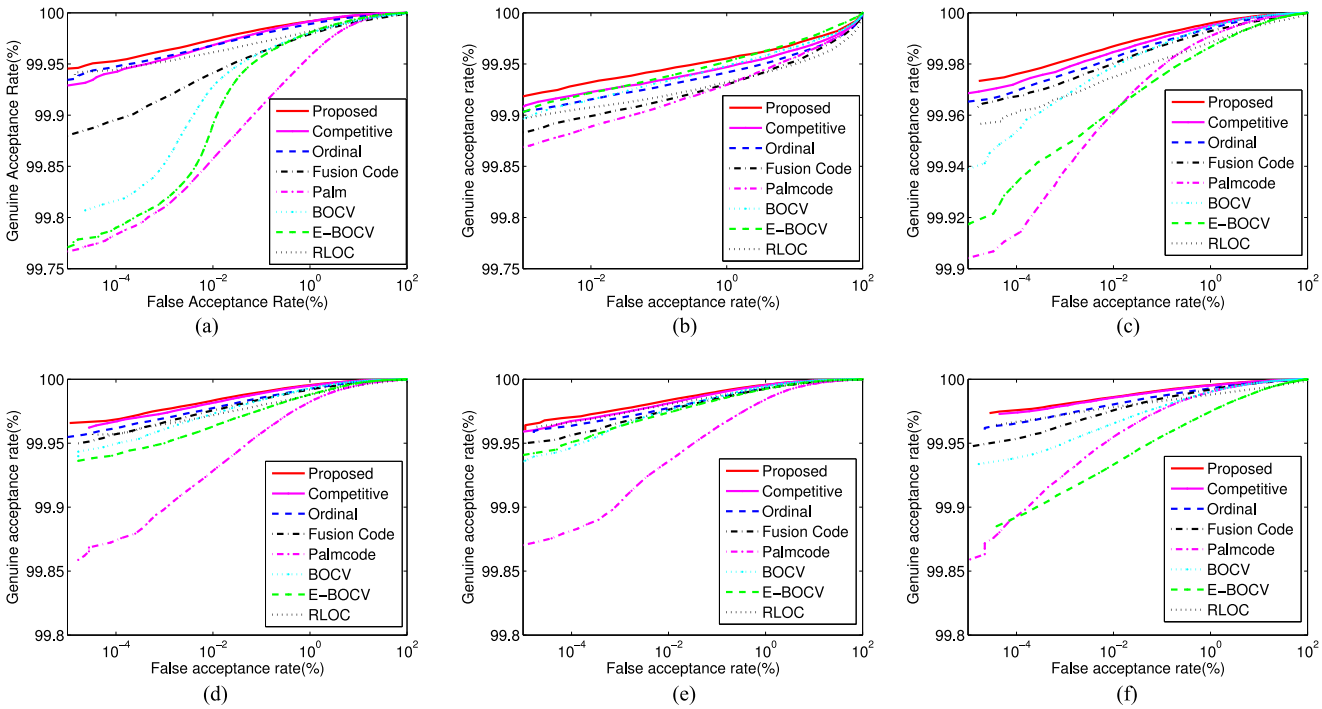

Fig. 9. ROC curves of different methods on different types of databases. (a)–(f) ROC curves on the PolyU, IITD, Red, Green, Blue, and NIR databases, respectively.

TABLE I
EER (%) OF DIFFERENT ORIENTATION-BASED METHODS ON THREE TYPES OF PALMPRINT DATABASES

EER	Competitive code	Ordinal code	Fusion code	Palmcode	BOCV	E-BOCV	RLOC	Proposed
PolyU	0.0261	0.0272	0.0899	0.0931	0.0469	0.0532	0.0360	**0.0225**
IITD	0.0696	0.0744	0.0878	0.0933	0.0708	0.0671	0.0826	**0.0594**
Red	0.0145	0.0161	0.0179	0.0297	0.0186	0.0131	0.0223	**0.0125**
Green	0.0168	0.0202	0.0216	0.0507	0.0232	0.0303	0.0249	**0.0152**
Blue	0.0170	0.0202	0.0212	0.0463	0.0207	0.0225	0.0203	**0.0152**
NIR	0.0137	0.0180	0.0213	0.0332	0.0284	0.0510	0.0208	**0.0134**

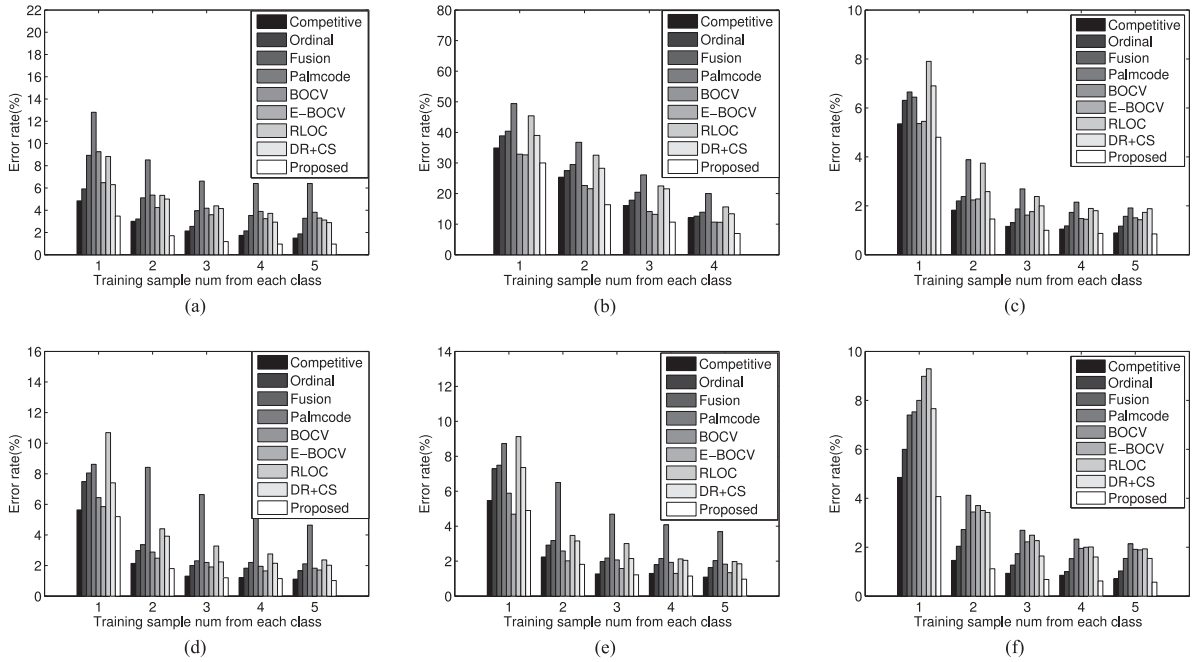

Fig. 10. Palmprint identification error rate. (a)–(f) Error rate on PolyU, IITD, Red, Green, Blue, and NIR databases, respectively.

TABLE II
ERROR RATE (%) OF PALMPRINT IDENTIFICATION WITH $N = 1$

Err	Competitive code	Ordinal code	Fusion code	Palmcode	BOCV	E-BOCV	RLOC	DR + CS	Proposed
PolyU	4.85	5.92	8.93	12.81	9.26	6.48	8.83	6.30	**3.48**
IITD	34.89	38.86	40.38	49.40	32.88	32.65	45.43	39.00	**30.00**
Red	5.35	6.31	6.65	6.44	5.36	5.45	9.90	7.41	**4.81**
Green	5.64	7.49	8.05	8.62	6.44	5.85	10.69	9.36	**5.20**
Blue	5.47	7.29	7.49	8.73	5.89	4.69	9.13	6.66	**4.90**
NIR	4.85	6.00	7.40	7.53	8	8.98	9.29	6.90	**4.07**

can better present the multiple dominant orientation features of the palmprint. The experimental results also corroborate the conclusion of [19] that by fusing different bands, rather than using a single band, the accuracy can be significantly increased. Further, the fusion of Blue, Red, and NIR bands gives the most competitive results on multispectral palmprint database.

E. Effectiveness in Rank-Level Fusion

For a better evaluation of the effectiveness of the neighboring direction indicator, we fused the proposed method with other matchers in rank level and compared the performance with that of the fusion scheme in [6], in terms of palmprint identification. In [6], by using various rank-level-combination methods, it fuse the matching results obtained by the palmcode, competitive code, and RLOC methods at rank level. Compared with [6], we fuse the proposed method with the palmcode and competitive code methods at rank level. This is mainly because both the competitive code and RLOC methods extract the dominant orientation feature of palmprint. In other words, the competitive code and RLOC share many redundant features of palmprint. In addition, the whole IITD database was employed in our

TABLE III
COMPARISON OF THE RESULTS OBTAINED BY FUSING MULTISPECTRAL BANDS

EER(%)	Method in [19]	The proposed method
Blue and Red	0.0130	**0.0117**
Blue, Red, and NIR	0.0096	**0.0088**
Blue, Red, Green, and NIR	0.0098	**0.0089**

TABLE IV
AVERAGE IDENTIFICATION ACCURACY RATE (%) OBTAINED BY USING DIFFERENT RANK-LEVEL FUSION SCHEMES

	Fusion scheme in [6]			The proposed fusion scheme		
	Borda count	$\sum e^{w_i R_i}$	$\sum w_i e^{R_i}$	Borda count	$\sum e^{w_i R_i}$	$\sum w_i e^{R_i}$
Rank1	87.91	88.60	88.69	91.08	92.60	92.65
Rank2	88.47	89.56	90.65	91.47	93.60	93.81
Rank3	89.30	91.08	91.30	91.95	94.13	95.04

TABLE V
EXPERIMENTAL RESULTS OBTAINED BY USING THE THIRD ORDINAL MEASUREMENT-BASED METHOD (%)

	PolyU	IITD	Red	Green	Blue	NIR
EER	0.0254	0.0635	0.0140	0.0160	0.0159	0.0154
Err rate ($N = 1$)	3.62	32.45	5.22	5.78	5.45	4.96
Err rate ($N = 2$)	1.82	18.33	1.64	2.04	2.06	1.70

experiments, where one image of each palmprint was selected as the test sample and the rest as the training samples. Each of the five palmprint images was used as the test sample, and thus, the experiments were performed five times and the average accurate rates reported. Using both linear (i.e., Borda Count) and nonlinear rank combination methods (i.e., weighted exponential function-based methods) [6], we performed a series comparison between the fusion scheme in [6] and the proposed fusion scheme. The parameters of three matchers in the weighted nonlinear rank combinations were empirically set to 0.1, 0.4, and 0.5. From a comparison of the identification results presented inTable IV, it is found that the proposed scheme consistently achieves better accuracy than the one in [6]. Therefore, the proposed method can be effectively fused with other matchers at rank level for palmprint identification.

F. Comparisons With Another Ordinal Measurement-Based Method

As mentioned in Section IV-D, the unified framework includes three kinds of ordinal measurement-based methods. In the foregoing experiments, we compared the proposed method with the conventional ordinal code method. In this section, we compare the proposed method with another ordinal measurement-based method, which represents the case of the unified framework with $k = 1$. The experimental results obtained by using the third ordinal measurement-based method are presented in Table V, from which it can be seen that their EERs and error rate in palmprint identification are higher than those of the proposed method. Therefore, we can conclude that, among the three kinds of ordinal measurement-based methods, the proposed method performs the best.

TABLE VI
COMPUTATIONAL COST OF DIFFERENT CODING METHODS

Methods	Featureextraction	Matching	Total
Proposed	39.899 ms	0.063 ms	39.962 ms
Competitive Code	38.540 ms	0.095 ms	38.635 ms
Ordinal Code	19.500 ms	0.080 ms	19.580 ms
Fusion Code	2.916 ms	0.084 ms	3.000 ms
Palmcode	1.760 ms	0.224 ms	1.984 ms
BOCV	39.718 ms	0.082 ms	39.800 ms
E-BOCV	40.636 ms	0.835 ms	41.471 ms
RLOC	67.137 ms	3.921 ms	71.058 ms

G. Computational Complexity

To evaluate the computational complexity of the proposed method, we compared its computational time with that of the current state-of-the-art coding methods. The current state-of-the art coding methods were also implemented for comparison. All the algorithms were conducted on a PC with double-core Intel(R) i5-3470 (3.2 GHz), RAM 8.00 GB, and Windows 7.0 operating system. MATLAB 8.1.0 is the software platform. To demonstrate the computational complexity explicitly, the computational cost of feature extraction and that of matching were calculated separately and both were calculated 1000 times. The average time taken for each stage was computed, and then, the total time cost summed up. Table VI summarizes the precise time consumed by different methods. From these results, it can be seen that the execution time taken in feature extraction by the proposed method is about 39.90 ms, which is close to that of the competitive code method. This is because the Gabor filtering part, which is the most computationally demanding in feature extraction, is the same. Considering that a simple and effective hamming distance matching scheme was used, the matching speed of the proposed method is slightly faster than that of the competitive code method. As a result, the total computational cost of the proposed method, which is about 40 ms, is comparable with that of the competitive code method. Further, the total time cost of our method is similar to that of the BOCV and E-BOCV methods.

VI. CONCLUSION

In this paper, we have investigated the relationship between two orientations of a palmprint to identify the more discriminative orientation and then used a group of neighboring direction indicators to represent the relation of these orientations. The neighboring direction indicator can not only essentially represent the most dominant orientation feature of the palmprint, but can also better denote the multiple orientations of some special points having double dominant orientations. In addition, a simple and effective smoothing convolution has been introduced to improve the precision of the orientation feature of the palmprint. Experimental results show that the proposed

method can achieve higher accuracy in palmprint recognition than the state-of-the-art orientation-based methods. Moreover, the proposed method gives the most competitive performance in multispectral palmprint verification.

REFERENCES

[1] A. Kong, D. Zhang, and M. Kamel, "A survey of palmprint recognition," *Pattern Recognit.*, vol. 42, no. 7, pp. 1408–1418, 2009.

[2] D. Zhang, *Advanced Pattern Recognition Technologies with Applications to Biometrics*. Hershey, PA, USA: Med. Inf. Sci. Ref., 2009.

[3] A. K. Jain, A. Ross, and S. Prabhakar, "An introduction to biometric recognition," *IEEE Trans. Circuits Syst. Video Technol.*, vol. 14, no. 1, pp. 4–20, Jan. 2004.

[4] A. K. Jain and J. Feng, "Latent palmprint matching," *IEEE Trans. Pattern Anal. Mach. Intell.*, vol. 31, no. 6, pp. 1032–1047, Jun. 2009.

[5] Q. Dai, N. Bi, and D. Huang, "M-band wavelets application to palmprint recognition based on texture features," in *Proc. Int. Conf. Image Process.*, 2004, pp. 893–896.

[6] A. Kumar and S. Shekhar, "Personal identification using multibiometrics rank-level fusion," *IEEE Trans. Syst., Man, Cybern. C, Appl. Rev.*, vol. 41, no. 5, pp. 743–752, Sep. 2011.

[7] J. Malik, D. Girdhar, and R. Dahiya, "Accuracy improvement in palmprint authentication system," *Int. J. Image, Graphics Signal Process.*, vol. 4, pp. 51–59, 2015.

[8] F. Yue, B. Li, and M. Yu, "Hashing based fast palmprint identification for large-scale databases," *IEEE Trans. Inf. Forensics Security*, vol. 8, no. 5, pp. 769–778, May 2013.

[9] D. S. Huang, W. Jia, and D. Zhang, "Palmprint verification based on principal lines," *Pattern Recognit.*, vol. 41, no. 4, pp. 1316–1328, 2008.

[10] X. Wu, D. Zhang, and K. Wang, "Palm line extraction and matching for personal authentication," *IEEE Trans. Syst., Man Cybern. A, Syst. Humans*, vol. 36, no. 5, pp. 978–987, Sep. 2006.

[11] D. Zhang, W.-K. Kong, J. You, and L. M. Wong, "Online palmprint identification," *IEEE Trans. Pattern Anal. Mach. Intell.*, vol. 25, no. 9, pp. 1041–1050, Sep. 2003.

[12] A. Morales, M. A. Ferrer, and A. Kumar, "Towards contactless palmprint authentication," *IET Comput. Vision*, vol. 5, pp. 407–416, 2011.

[13] J. Dai, J. Feng, and J. Zhou, "Robust and efficient ridge-based palmprint matching," *IEEE Trans. Pattern Anal. Mach. Intell.*, vol. 34, no. 8, pp. 1618–1632, Aug. 2012.

[14] F. Chen, X. Huang, and J. Zhou, "Hierarchical minutiae matching for fingerprint and palmprint identification," *IEEE Trans. Image Process.*, vol. 22, no. 12, pp. 4964–4971, Dec. 2013.

[15] E. Liu, A. K. Jain, and J. Tian, "A coarse to fine minutiae-based latent palmprint matching," *IEEE Trans. Pattern Anal. Mach. Intell.*, vol. 35, no. 10, pp. 2307–2322, Oct. 2013.

[16] V. Roux, S. Aoyama, K. Ito, and T. Aoki, "Performance improvement of phase-based correspondence matching for palmprint recognition," in *Proc. IEEE Conf. Comput. Vision Pattern Recognit.*, 2014, pp. 70–77.

[17] G. S. Badrinath and P. Gupta, "Palmprint based recognition system using phase-difference information," *Future Gener. Comput. Syst.*, 2012, pp. 287–305.

[18] W. Li, L. Zhang, D. Zhang, G. Lu, and J. Yan, "Efficient joint 2D and 3D palmprint matching with alignment refinement," in *Proc. IEEE Conf. Comput. Vision Pattern Recognit.*, 2010, pp. 795–801.

[19] D. Zhang, Z. Guo, G. Lu, L. Zhang, and W. Zuo, "An online system of multi-spectral palmprint verification," *IEEE Trans. Instrum. Meas.*, vol. 59, no. 2, pp. 480–490, Feb. 2010.

[20] R. Raghavendra and C. Busch, "Novel image fusion scheme based on dependency measure for robust multispectral palmprint recognition," *Pattern Recognit.*, vol. 47, pp. 2205–2221, 2014.

[21] Y. Xu, L. Fei, and D. Zhang, "Combing left and right palmprint image for more accurate personal identification," *IEEE Trans. Image Process.*, vol. 24, no. 2, pp. 549–559, Feb. 2015.

[22] J. Dai and J. Zhou, "Multifeature-based high-resolution palmprint recognition," *IEEE Trans. Pattern Anal. Mach. Intell.*, vol. 33, no. 5, pp. 945–957, May 2011.

[23] S. Ribaric and I. Fratric, "A biometric identification system based on eigenpalm and eigenfinger features," *IEEE Trans. Pattern Anal. Mach. Intell.*, vol. 27, no. 11, pp. 1698–1709, Nov. 2005.

[24] X. Wu, D. Zhang, and K. Wang, "Fisherpalms based palmprint recognition," *Pattern Recognit. Lett.*, vol. 24, pp. 2829–2838, 2003.

[25] D. Hu, G. Feng, and Z. Zhou, "Two-dimensional locality preserving projections (2DLPP) with its application to palmprint recognition," *Pattern Recognit.*, vol. 24, pp. 339–342, 2007.

[26] T. Connie, A. Jin, M. Ong, and D. Ling, "An automated palmprint recognition system," *Image Vision Comput.*, vol. 23, no. 5, pp. 501–515, 2005.

[27] A. W. K. Kong and D. Zhang, "Competitive coding scheme for palmprint verification," in *Proc. 17th Int. Conf. Pattern Recognit.*, 2004, pp. 520–523.

[28] A. Kong, D. Zhang, and M. Kamel, "Palmprint identification using feature-level fusion," *Pattern Recognit.*, vol. 39, pp. 478–487, 2006.

[29] W. Jia, D. Huang, and D. Zhang, "Palmprint verification based on robust line orientation code," *Pattern Recognit.*, vol. 41, pp. 1504–1513, 2008.

[30] W. Zuo, Z. Lin, Z. Guo, and D. Zhang, "The multiscale competitive code via sparse representation for palmprint verification," in *Proc. IEEE Conf. Comput. Vision Pattern Recognit.*, 2010, pp. 2265–2272.

[31] Z. Guo, D. Zhang, L. Zhang, and W. Zuo, "Palmprint verification using binary orientation co-occurrence vector," *Pattern Recognit. Lett.*, vol. 30, pp. 1219–1227, 2009.

[32] L. Zhang, H. Li, and J. Niu, "Fragile bits in palmprint recognition," *IEEE Signal Process. Lett.*, vol. 19, no. 10, pp. 663–666, Oct. 2012.

[33] Z. Sun, T. Tan, Y. Wang, and S. Li, "Ordinal palmprint representation for personal identification," *Comput. Vision Pattern Recognit.*, vol. 1, pp. 279–284, 2005.

[34] H. K. Kalluri, M. Prasad, and A. Agarwal, "Palmprint identification and verification based on wide principal lines through dynamic ROI," *Int. J. Biometrics*, vol. 7, no. 1, pp. 1–30, 2015.

[35] H. Li, J. Dong, and J. Li, "Novel palmprint representations for palmprint recognition," in *Proc. 17th Int. Conf. Mach. Vision*, 2015, pp. 944505-1–944505-5.

[36] V. Deemter, J. H. Du, and J. M. H. Buf, "Simultaneous detection of lines and edges using compound Gabor filters," *Pattern Recognit. Artif. Intell.* vol. 14, pp. 757–777, 2000.

[37] T. S. Lee, "Image representation using 2D Gabor wavelets," *IEEE Trans. Pattern Anal. Mach. Intell.*, vol. 18, no. 10, pp. 959–971, Oct. 1996.

[38] F. Xue, W. Zuo, and K. Wang, "A performance evaluation of filter design and coding schemes for palmprint recognition," in *Proc. 19th Int. Conf. Pattern Recognit.*, 2008, pp. 1–4.

[39] PolyU palmprint database (version 2.0), Multispectral palmprint database. (2003). [Online]. Available: http://www.comp.polyu.edu.hk/∼biometrics/

[40] IITD Touchless Palmprint Database(version1.0). (2007). [Online]. Available: http://www4.comp.polyu.edu.hk/∼csajaykr/IITD/Database_Palm.htm

Lunke Fei (S'15) received the B.S. and M.S. degrees in computer science and technology from East China Jiaotong University, Nanchang, China, in 2004 and 2007, respectively. He is currently working toward the Ph.D. degree in computer science and technology at the Shenzhen Graduate School, Harbin Institute of Technology, Shenzhen, China.

His current research interests include biometrics, pattern recognition, and image processing.

Bob Zhang (M'12) received the B.A. degree in computer science from York University, Toronto, ON, Canada, in 2006, the M.A.Sc. degree in information systems security from Concordia University, Montreal, QC, Canada, in 2007, and the Ph.D. degree in electrical and computer engineering from the University of Waterloo, Waterloo, ON, Canada, in 2011.

After graduating from the University of Waterloo, he remained with the Center for Pattern Recognition and Machine Intelligence. He was a Postdoctoral Researcher with the Department of Electrical and Computer Engineering, Carnegie Mellon University, Pittsburgh, PA, USA. He is currently an Assistant Professor with the Department of Computer and Information Science, University of Macau, Taipa, Macau. His research interests include biometrics, pattern recognition, and image processing.

Dr. Zhang is a Technical Committee Member of the IEEE Systems, Man, and Cybernetics Society, an Associate Editor for the *International Journal of Image and Graphics*, and an Editorial Board Member for the *International Journal of Information*.

Yong Xu (SM'15) received the B.S. and M.S. degrees in 1994 and 1997, respectively, and the Ph.D. degree in pattern recognition and intelligence system in 2005, all from the Nanjing University of Science and Technology, Nanjing, China.

He is currently with the Bio-Computing Research Center, Shenzhen Graduate School, Harbin Institute of Technology, Shenzhen, China. His current research interests include pattern recognition, biometrics, bioinformatics, machine learning, image processing, and video analysis.

Liping Yan received the B.S. and M.S. degrees in computer science and technology from East China Jiaotong University, Nanchang, China, in 2001 and 2007, respectively. She is currently working toward the Ph.D. degree in computer science and technology at the Computer School, Wuhan University, Wuhan, China.

Her current research interests include pattern recognition and intelligent transportation systems.